

# Effects of Two Different Maleic Anhydride-Modified Adhesion Promoters (PP-g-MA) on the Structure and Mechanical Properties of Nanofilled Polyolefins

P. Eteläaho, K. Nevalainen, R. Suihkonen, J. Vuorinen, P. Järvelä

Laboratory of Plastics and Elastomer Technology, Tampere University of Technology,  
Korkeakoulunkatu 6, 33720 Tampere, Finland

Received 20 March 2008; accepted 8 March 2009

DOI 10.1002/app.30394

Published online 16 June 2009 in Wiley InterScience (www.interscience.wiley.com).

**ABSTRACT:** The effects of adhesion promoter properties on the structure and mechanical behavior of nanoclay-filled polyolefin nanocomposites are presented. Two different maleic anhydride-modified polypropylenes having varying maleic anhydride content and molecular weight were used. The influence of these parameters on the performance and morphology of the prepared polypropylene and high density polyethylene-based nanocomposites was examined by mechanical testing, X-ray diffraction, and electron microscopy. The low molecular weight adhesion promoter seemed to be effective in both matrices in relation to mechanical property enhancements, whereas its high molecular weight counter-

part performed well only in polyethylene matrix. X-ray diffraction results and examination of morphology revealed that the intercalation and the dispersion of the nanoclay were more even in both matrices when the low molecular weight adhesion promoter with a higher maleic anhydride content was used. On the other hand, the use of high molecular weight adhesion promoter led to a less uniform dispersion but also to a greater amount of exfoliated clay particles. © 2009 Wiley Periodicals, Inc. *J Appl Polym Sci* 114: 978–992, 2009

**Key words:** adhesion; morphology; nanocomposites; organoclay; polyolefins

## INTRODUCTION

It is commonly known that when preparing polyolefin-based nanocomposites, especially with melt compounding technology, the successful choice and utilization of adhesion promoters are very important when it comes to the morphological quality and properties of the prepared nanocomposites.

Polyolefins, such as polypropylene (PP) and polyethylene (PE) in particular, are challenging as matrix materials because of their strong hydrophobicity. In nanoclay-filled composites, this characteristic feature impairs the possibility of proper clay dispersion and exfoliation because of the opposing hydrophilic nature of clay fillers. This contradiction is usually attempted to be overcome by the surface modification of filler particles and utilization of adhesion promoters to make the matrix and filler more compatible. Maleic anhydride-modified polyolefins have proven to be effective adhesion-promoting agents in polyolefin-based nanocomposites already a decade ago,<sup>1–3</sup> but they are still under intense research. There are various grades available in this family of adhesion promoters, which differ from each other in terms of their main chain, molecular weight, and

maleic anhydride content. Still, there appear various opinions about the effects of these parameters on polyolefin-based nanocomposite structure and nanoclay dispersion as well as the gained property enhancements.<sup>4–8</sup>

The functioning of maleic anhydride-modified polyolefins, such as those based on polypropylene (PP-g-MA) or polyethylene (PE-g-MA), is dependent on two factors. First, the maleic anhydride content determines the ability of the adhesion promoter to form chemical bonds with the surface chemistry of the nanoclay particles. Second, the molecular weight and the main chain of the adhesion promoter determine the accessibility of the adhesion promoter between the individual clay layers to induce intercalation and exfoliation as well as miscibility with the polymer matrix.<sup>1</sup> Miscibility is a very important factor in terms of exfoliation possibilities, i.e., if the miscibility of the adhesion promoter and the polymer matrix is good, exfoliation should quite easily follow after successful intercalation. If miscibility presents a problem, phase separation occurs with no exfoliation. Therefore, molecular weight and maleic anhydride content are parameters that contribute strongly to the morphology and the adhesion achieved in the composite.

In this study, two types of maleic anhydride-modified polypropylenes (PP-g-MA) were studied in two polyolefin matrices, polypropylene (PP) and

Correspondence to: P. Eteläaho (pirkko.etelaaho@tut.fi).

TABLE I  
Material Details

Material	Trade name	Supplier	Density [g/cm <sup>3</sup> ]	Melt flow rate [g/10 min]	M <sub>n</sub> [g/mol]
PP	HF700SA	Borealis	0.908	21	–
PE-HD	CG8410	Borealis	0.941	7.5	–
PP-g-MA	Licomont AR 504	Clariant	–	–	1,500–2,900
PP-g-MA	Scona TPPP 2112 FA	Kometra	–	–	200,000–300,000
Nanoclay	Nanomer I.44P	Nanocor	1.7	–	–

high density polyethylene (PE-HD). The effect of the maleic anhydride content and molecular weight of the adhesion promoters were evaluated in terms of their ability to enhance clay dispersion, adhesion, and mechanical properties in both matrices. It was interesting to study how these varying parameters affect nanoclay dispersion and property enhancements in a single matrix and in turn, if they have the same effect when the matrix polymer is changed.

## EXPERIMENTAL

### Materials

Two different adhesion promoters were used in this study, which are both maleic anhydride-modified polypropylenes but differ from each other in terms of molecular weight and maleic anhydride content. Clariant's Licomont AR 504 has a low molecular weight ( $M_n = 1,500\text{--}2,900$  g/mol) and maleic anhydride content of 3.5–4%,<sup>9,10</sup> whereas Kometra's Scona TPPP 2112 FA has a notably higher molecular weight ( $M_n = 200,000\text{--}300,000$  g/mol) and lower maleic anhydride content of approximately only 1%. The nanoclay Nanomer I.44P (Nanocor) was chosen according to its known suitability for polyolefin matrices. It has an average particle size of 15–20  $\mu\text{m}$  and a quaternary ammonium chemistry-based surface

modification. This nanoclay and both aforementioned adhesion promoters were used to produce nanocomposites in two polyolefin matrices, PP (HF700SA) and PE-HD (CG8410), which were both supplied by Borealis. The used PP is a general purpose injection molding grade having a medium melt flow rate, whereas the PE-HD grade has a substantially lower melt flow rate, as its primary application area is extrusion. Application of PP-g-MA was justified also in PE-HD matrix because, for instance, Lee et al.<sup>11</sup> have gained a better exfoliation degree with PP-g-MA than with PE-g-MA in PE-HD-based nanocomposites. Characteristic details of the used materials are listed in Table I.

### Preparation of the nanocomposites

The nanocomposites were prepared with a co-rotating Brabender DSE 25 twin-screw extruder at a screw speed of 200 rpm. For both studied matrices, the temperature profile in the cylinder was 170-170-170-170-170-180-180-185°C from feeder to die. Before processing, nanoclay was dried for 24 h at 80°C. The content of nanoclay was 3, 6, and 8 wt %, although the amount of adhesion promoter was kept constant (9 wt %). Compounds containing mere nanoclay or adhesion promoter were also made for reference. Tables II and III reveal the compositions of the prepared nanocomposites.

TABLE II  
Compositions of the PP-Based Nanocomposites

Abbreviation	PP	Nanomer	Licomont	Scona TPPP
	[wt %]	I.44P [wt %]	AR 504 [wt %]	2112 FA [wt %]
PP	100	–	–	–
PP-LIC	91	–	9	–
PP-SCO	91	–	–	9
PP-3	97	3	–	–
PP-6	94	6	–	–
PP-8	92	8	–	–
PP-3-LIC	88	3	9	–
PP-6-LIC	85	6	9	–
PP-8-LIC	83	8	9	–
PP-3-SCO	88	3	–	9
PP-6-SCO	85	6	–	9
PP-8-SCO	83	8	–	9

TABLE III  
Compositions of the PE-HD-Based Nanocomposites

Abbreviation	PE-HD	Nanomer	Licomont	Scona TPPP
	[wt %]	I.44P [wt %]	AR 504 [wt %]	2112 FA [wt %]
PE-HD	100	–	–	–
PE-LIC	91	–	9	–
PE-SCO	91	–	–	9
PE-3	97	3	–	–
PE-6	94	6	–	–
PE-8	92	8	–	–
PE-3-LIC	88	3	9	–
PE-6-LIC	85	6	9	–
PE-8-LIC	83	8	9	–
PE-3-SCO	88	3	–	9
PE-6-SCO	85	6	–	9
PE-8-SCO	83	8	–	9

**TABLE IV**  
Crystallization Behavior of the PP-Based Nanocomposites

Material	T <sub>m, peak</sub> [°C]	ΔH <sub>f</sub> [J/g]	Crystallinity [%]
PP	170.40	80.72	39
LICOMONT	150.70	46.66	23
SCONA	164.30	84.98	41
PP-LIC	169.10	77.50	37
PP-SCO	171.30	79.46	38
PP-3	170.50	98.69	49
PP-6	169.70	85.99	44
PP-8	169.20	89.28	47
PP-3-LIC	170.50	81.15	40
PP-6-LIC	168.40	70.45	36
PP-8-LIC	168.40	71.31	37
PP-3-SCO	168.84	77.26	38
PP-6-SCO	169.20	72.95	37
PP-8-SCO	168.34	74.42	39

### Characterization methods

Crystallization behavior of the materials was studied through Netzch 204 F1 DSC scans at a heating rate of 10°C/min. The melting temperature (T<sub>m,peak</sub>), heat of fusion (ΔH<sub>f</sub>), and crystallinity degree were determined for each compound. The percent crystallinity (X) of the polymer matrix was calculated according to the following formula:

$$X = \frac{\Delta H_f}{f_p \Delta H_f^0} \times 100\% \quad (1)$$

where ΔH<sub>f</sub> is the heat of fusion of the polymer matrix, f<sub>p</sub> is the weight fraction of the polymer matrix, and ΔH<sub>f</sub><sup>0</sup> is the heat of fusion for 100% crystalline polymer. The used values for ΔH<sub>f</sub><sup>0</sup> were 207.1 J/g for PP<sup>12</sup> and 293 J/g for PE-HD.<sup>13</sup>

The compounds were characterized for mechanical performance by conducting both tensile and impact tests. The test bars congruent with ISO 527 were made with a Krauss Maffei KM50C2 injection molding machine after drying the materials for 6 h at 80°C. Tensile tests were performed according to ISO 527 with a Messphysik Midi 10-20 universal testing machine at a test speed of 50 mm/min. The impact test behavior of the materials was determined according to ISO 179 with a Ceast Resil 5.5 J impact tester by applying a 4 J hammer for the unnotched and a 0.5 J hammer for the notched specimens. The fracture surfaces of the gold-coated impact test specimens were examined with a Philips XL-30 scanning electron microscope (SEM) at an acceleration voltage of 15 kV to evaluate the possible differences in fracture behavior and to analyze clay dispersion.

In addition, the quality of dispersion as well as intercalation and exfoliation levels of the nanoclay were examined by X-ray diffraction (XRD) and transmission electron microscopy (TEM). Siemens D-

500 XRD equipment was used to carry out the XRD measurements with CuKα radiation (λ = 1.5406 Å). The scanning was performed in the 2θ range of 1–8° at a scanning rate of 0.3°/min for all the nanocomposites and 0.2°/min for the pure montmorillonite reference (MMT). TEM images were taken with Philips FEI Tecnai F12 and JEOL model JEM 2010 at an acceleration voltage of 120 kV. The specimens were about 100–120 nm thick and prepared with a Leica Ultracut UCT ultramicrotome at room temperature. To improve contrast, the samples were poststained with uranyl acetate and lead citrate.

## RESULTS AND DISCUSSION

### Crystallization behavior, mechanical properties, and fracture surface analysis

Crystallization data of the PP- and PE-HD-based compounds is gathered up in Tables IV and V, respectively. Neat Licomont and neat Scona are also included for reference. The melting temperatures and heats of fusion were quite close to each other for neat PP and neat Scona, which led to crystallinity degrees of about 40%, as shown in Table IV. In turn, neat Licomont had a lower melting temperature and a notably lower heat of fusion resulting in a much lower degree of crystallinity, which was expected because of its low molecular weight. However, when adhesion promoters were compounded with PP, the melting behavior and crystallinity were nearly similar for compounds, PP-LIC and PP-SCO, and approaching the results obtained for neat PP. There were no marked differences in the melting behavior and crystallinity for compounds containing both clay and adhesion promoter, but a slight increase in crystallinity was observed for compounds containing mere clay. This can be because of

**TABLE V**  
Crystallization Behavior of the PE-HD-Based Nanocomposites

Material	T <sub>m, peak</sub> [°C]	ΔH <sub>f</sub> [J/g]	Crystallinity [%]
PE-HD	135.80	145.90	50
LICOMONT	150.70	46.66	23
SCONA	164.30	84.98	41
PE-LIC	133.87	116.28	40
PE-SCO	134.17	117.65	40
PE-3	133.87	121.28	43
PE-6	133.37	133.75	49
PE-8	134.53	125.86	47
PE-3-LIC	134.20	102.91	36
PE-6-LIC	133.53	103.38	38
PE-8-LIC	134.34	107.70	40
PE-3-SCO	135.03	118.73	42
PE-6-SCO	135.03	118.76	43
PE-8-SCO	135.00	118.91	44

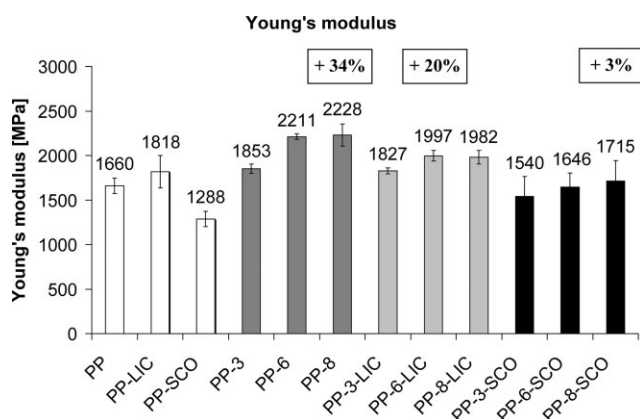


**Figure 1** Young's modulus of the PP-based nanocomposites. The percentual values describe the difference compared to the neat PP reference.

the nucleation effect of clay agglomerates observed in SEM analysis later on in this article.

In PE-HD-based compounds, the crystallinity degrees of the compounds, PE-LIC and PE-SCO, were somewhat lower than that for neat PE-HD because both adhesion promoters are PP-based (Table V). However, the melting temperatures were quite close to each other for PE-HD, PE-LIC, and PE-SCO and, in fact, for all compounds. The diminution of crystallinity was more pronounced in compounds containing clay and Licomont than in compounds containing clay and Scona. Furthermore, in case of PE-HD, the highest crystallinity among the nanoclay-filled compounds was gained when no adhesion promoter was included in the composition.

In tensile tests, the only significant changes in both matrices were seen in Young's modulus (Figs. 1, 2) whereas tensile strength and elongation at yield remained nearly unchanged, regardless of nanoclay content or adhesion promoter selection. Surprisingly, the mere addition of low molecular weight adhesion promoter (PP-LIC) led to a slight increase of Young's modulus in PP matrix, whereas an equal addition of high molecular weight Scona (PP-SCO) lowered the modulus value, as seen in Figure 1. The reason for this is unclear, for the predicted behavior should have been the other way around because, according to crystallization data, the molecular characteristics of Scona are closer to that of the matrix polymer (Table IV).

Figure 1 shows that the highest Young's modulus values were reached with mere nanoclay addition, the increase being above 30% at its best (PP-8). This might be partly explained by the higher crystallinity degrees obtained for the compounds containing only clay compared with those including both clay and adhesion promoter (Table IV). On the other hand, the stiffening effect of nanoclay may be partially lost simply because of the addition of low molecular

weight substances such as PP-g-MA, as the results in Figure 1 demonstrate. Ton-That et al.<sup>4</sup> and Wang et al.,<sup>5</sup> for instance, have also found out that the use of low molecular weight adhesion promoters impairs mechanical performance. However, for instance, Reichert et al.<sup>7</sup> have come to an opposite conclusion, i.e., the gained modulus values were usually lower for the compounds possessing no adhesion promoter compared with those in which a low molecular weight PP-g-MA was present. In our study, the change in Young's modulus was still notable (around 20%) when the adhesion promoter having a higher maleic anhydride content (Licomont) was used, but the application of Scona did not lead to any significant alteration in the modulus value as seen in Figure 1. The deviation was also larger for compounds containing Scona suggesting weak adhesion and uneven nanoclay dispersion. As an additive having high molecular weight and low maleic anhydride content, Scona would probably need more time and higher shear forces, i.e., longer mixing time, to function effectively in the chosen matrix and to reach a satisfying level of adhesion.

In the PE-HD matrix, the tensile test behavior concerning changes in Young's modulus was quite different (Fig. 2). Still, the changes in tensile strength and elongation at yield were as modest as in the PP matrix. The addition of Scona resulted in an increase of modulus (PE-SCO), whereas Licomont had a minor lowering effect on the modulus value (PE-LIC), as can be seen from Figure 2. In nanoclay-filled compounds, the increase in modulus was around 20% when no adhesion promoter was used. This stiffening effect was further enhanced when either of the adhesion promoters was used, resulting in elevations as high as 40%. Lee et al.<sup>11</sup> have reported increases in modulus of the same magnitude with 7 wt % clay and PP-g-MA use in PE-HD matrix, and also Gopakumar et al.<sup>14</sup> have achieved higher

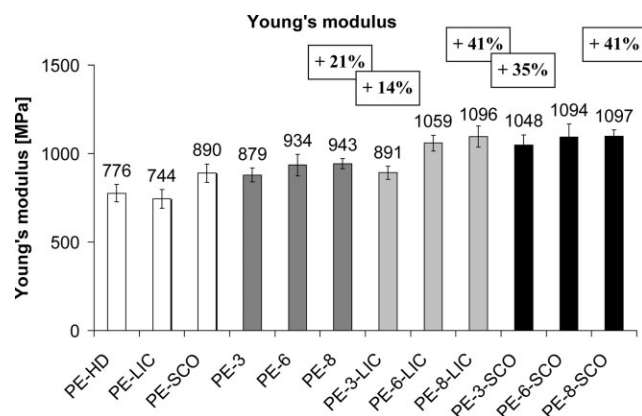


**Figure 2** Young's modulus of the PE-HD-based nanocomposites. The percentual values describe the difference compared to the neat PE-HD reference.

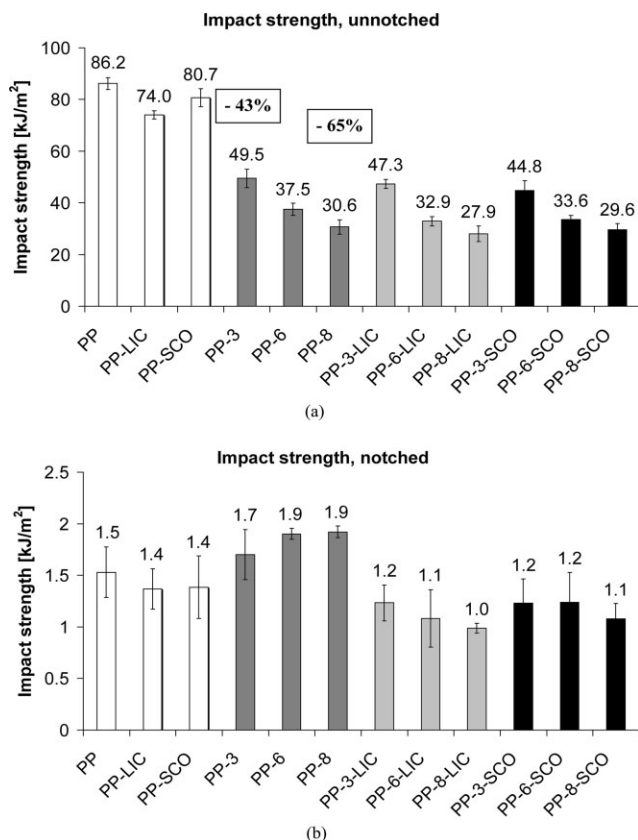


**Figure 3** Impact strengths of the PP-based nanocomposites: a) unnotched impact strengths and b) notched impact strengths. The percentual values describe the difference compared to the neat PP reference.

enhancements in modulus when adhesion promoter is included in the nanocomposite as well. An interesting phenomenon was that when Scona was used, already the lowest clay loading of 3 wt % led to an increase of more than 30% in modulus (PE-3-SCO). With PE-3-LIC, the effect was notably smaller. This might be because of the fact that since the addition of mere low molecular weight adhesion promoter (Licomont) had a slight lowering effect on Young's modulus, it is compensated only at higher clay loadings. Overall, the percentual changes in modulus values are more pronounced in PE-HD than in PP matrix, probably partly because of the fact that neat PE-HD has substantially lower Young's modulus, which is then more easily affected by filler addition.

Impact strengths of the materials were also determined. For the PP matrix, both unnotched and notched samples were tested, and the results are presented in Figure 3(a,b). Mere adhesion promoter addition decreased unnotched impact strength slightly, and the effect was in the same range regardless of adhesion promoter type (PP-LIC and PP-SCO). Nanoclay addition induced a more distinct decrease of unnotched impact strength, being more than 40% at a clay loading of 3 wt % (PP-3) and

more than 60% at a clay loading of 8 wt % (PP-8). The nanocomposites having both nanoclay and adhesion promoter in their composition behaved similarly compared with those containing mere clay. Consequently, no significant adhesion promoter type-based differences were noticeable from the obtained results. The fracture surfaces of the unnotched impact test specimens were also examined with a SEM, but no distinct changes in fracture mechanism between the compounds at similar clay concentrations were detected.

The notched impact strengths [Fig. 3(b)] revealed similar behavior when adhesion promoters were used: a mere adhesion promoter addition led to a small decrease in impact strength, whereas the change was more evident when clay was also included in the composition. Again, there were no significant discrepancies between the two adhesion promoters. More interesting behavior was noticed in the composites containing mere clay: the notched impact strengths were higher than that for neat PP. In general, increase in impact strength is known to be a sign of good adhesion and strong interactions between the composite constituents.<sup>15–17</sup> Reichert et al.<sup>7</sup> and Li et al.<sup>18</sup> have come to the same conclusion that notched impact strength (Izod) values are higher for the compounds that contain mere clay than for the pure PP reference or when adhesion promoter is also used. However, Li et al.<sup>18</sup> have noticed a strong deterioration of impact strength at higher clay concentrations than 4 wt %, whereas our results show otherwise.

Through SEM analysis, pronounced differences in fracture surface morphology of the notched impact test specimens were now observable between the compounds containing mere clay or clay together with adhesion promoter. As an example, SEM images at 6 wt % clay concentration are presented in Figure 4(a–c) at a magnification of 15 and in Figure 5(a–c) at a magnification of 100. It is clearly seen from Figure 4(a–c) that the fracture surface is rougher when mere clay is included in the composition. This is an indication of higher strength and clay particles efficiently disturbing crack propagation. The hindering of crack growth seems to be more effective without adhesion promoter, because the notched impact strength is higher when only clay is included in the composition. Explanations to the higher impact strengths achieved by mere clay addition could be weak dispersion or weak adhesion in the composites containing adhesion promoters, or the deteriorating effect of the adhesion promoter addition on the mechanical properties because of the adhesion promoter content, 9 wt %, which is relatively high. Reichert et al.<sup>7</sup> have also analyzed that this phenomenon could be because of the high concentration of low molecular weight PP-g-MA.

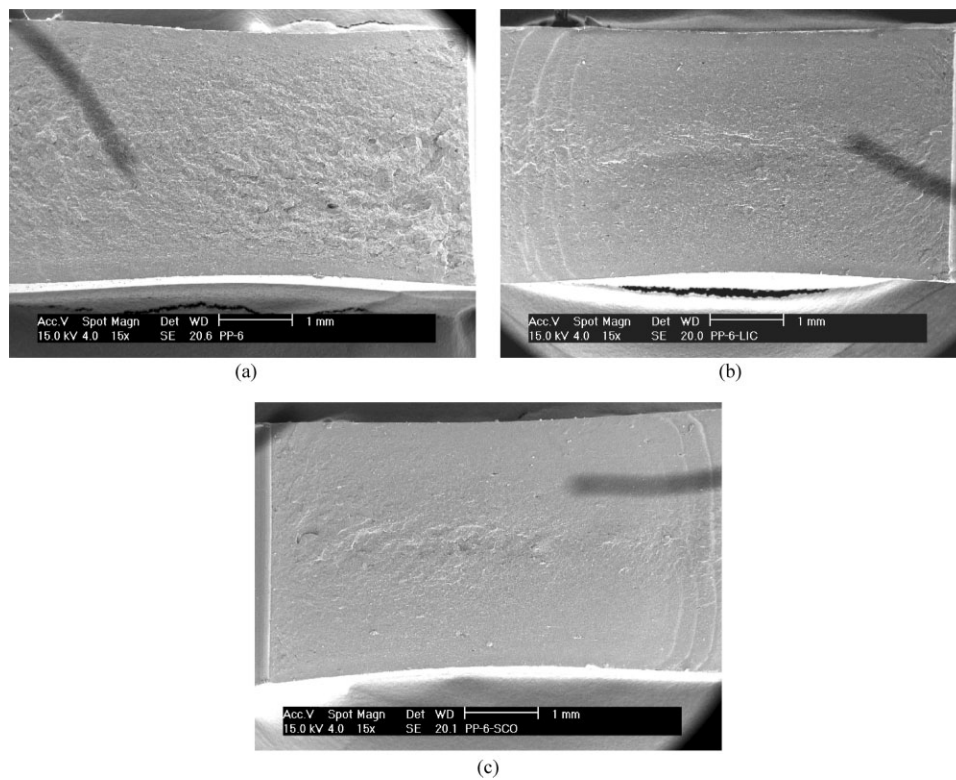


**Figure 4** SEM images taken from the fracture surfaces of the notched PP-based impact test specimens at a clay loading of 6 wt %: a) PP-6 15 $\times$ , b) PP-6-LIC 15 $\times$ , and c) PP-6-SCO 15 $\times$ .

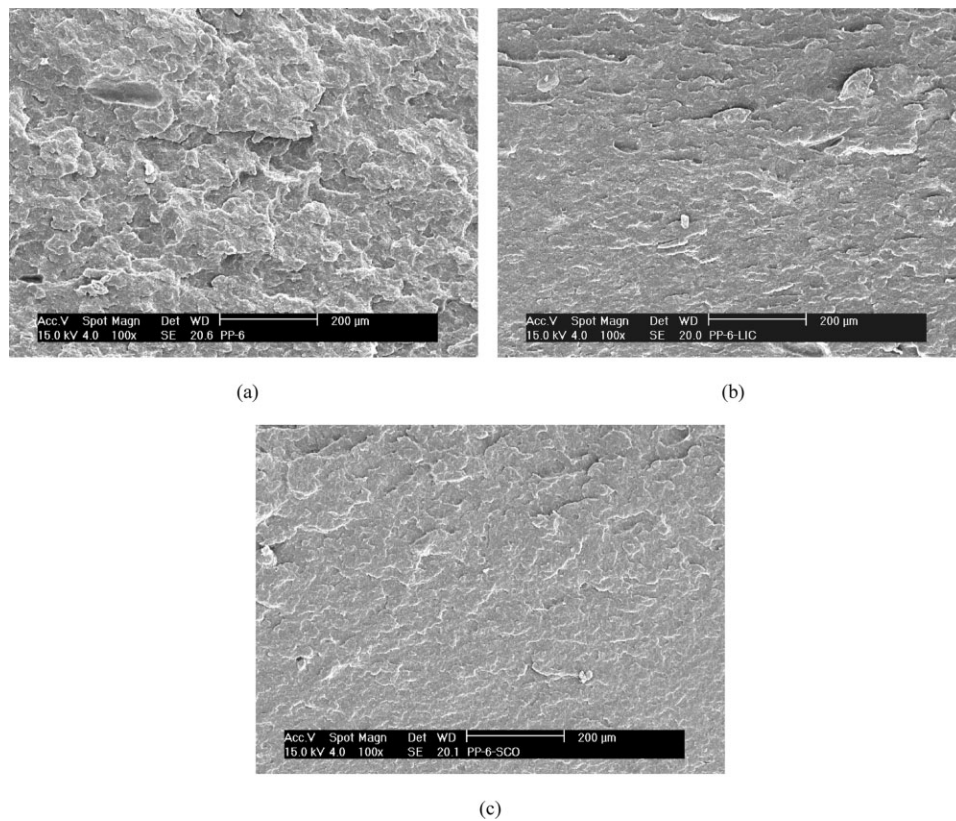


**Figure 5** SEM images taken from the fracture surfaces of the notched PP-based impact test specimens at a clay loading of 6 wt %: a) PP-6 100 $\times$ , b) PP-6-LIC 100 $\times$ , and c) PP-6-SCO 100 $\times$ .

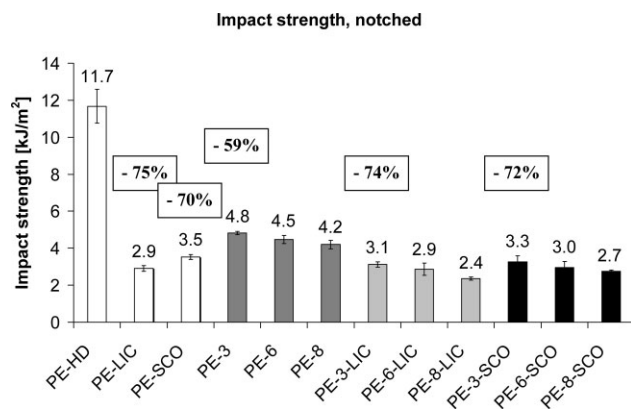


**Figure 6** Notched impact strengths of the PE-HD-based nanocomposites. The percentual values describe the difference compared to the neat PE-HD reference.

Focusing on clay dispersion, Figure 5(a–c) reveals the presence of larger agglomerates in compounds PP-6 and PP-6-LIC in comparison to PP-6-SCO, which is also observed in the corresponding XRD curves and TEM images [Figs. 11, 13(a–c)].

PE-HD is a very tough material, so the addition of adhesion promoters and clay easily produces a deleterious effect on (notched) impact strength, which is clearly detectable from Figure 6. However, in our research, unnotched samples of PE-HD were so

tough that they did not break with a 4 J hammer even when the clay concentration was 8 wt %. Mere nanoclay addition decreases the notched impact strength around 60% or more, whereas the effect of PP-based adhesion promoters is even more intense: notched impact strength drops down by 70%. This is the most substantial reason why the compounds containing both clay and adhesion promoters have notably lower impact strengths than those which contain only clay. In addition, fracture surface analysis of the notched impact test specimens revealed differences between the compounds at similar clay concentrations. SEM images at 8 wt % clay concentration are presented in Figure 7(a–c) at a magnification of 15 and in Figure 8(a–c) at a magnification of 100. PE-8-LIC shows a more plastic deformation compared with PE-8 and PE-8-SCO [Fig. 7(a–c)] and also distinguishes itself from others by the lack of large agglomerates [Fig. 8(a–c)]. The existence of larger agglomerates for PE-8 and PE-8-SCO is also evidenced in Figure 17, in which the XRD curves for the same compounds are presented. It is also clearly seen by comparing Figure 7(a–c) that the fracture surface of PE-8 is rougher than those of PE-8-LIC and PE-8-SCO, indicating higher resistance to crack propagation. This can be seen as somewhat higher notched impact strength in Figure 6.

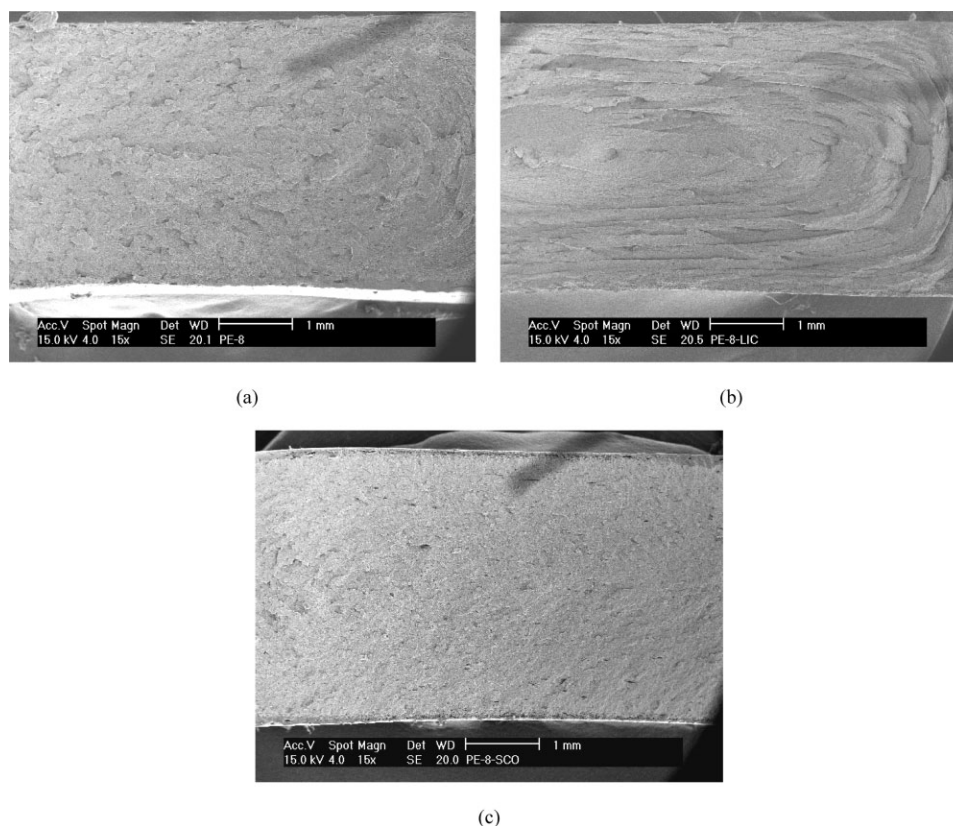


**Figure 7** SEM images taken from the fracture surfaces of the notched PE-HD-based impact test specimens at a clay loading of 8 wt %: a) PE-8 15 $\times$ , b) PE-8-LIC 15 $\times$ , and c) PE-8-SCO 15 $\times$ .

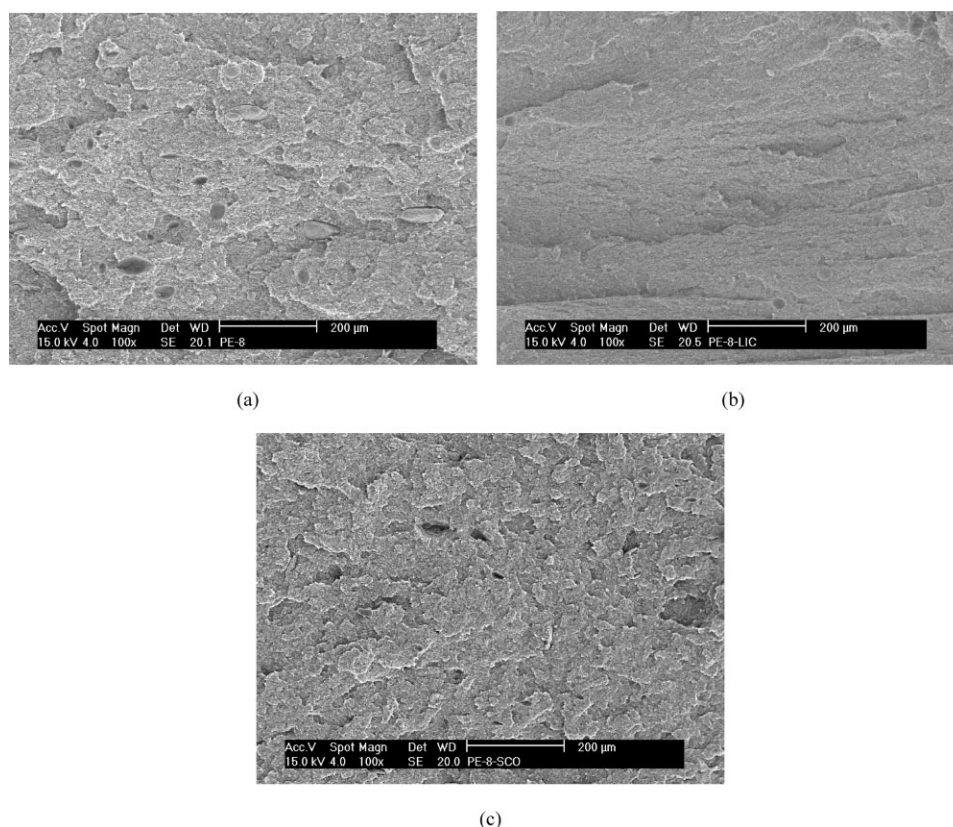


**Figure 8** SEM images taken from the fracture surfaces of the notched PE-HD-based impact test specimens at a clay loading of 8 wt %: a) PE-8 100 $\times$ , b) PE-8-LIC 100 $\times$ , and c) PE-8-SCO 100 $\times$ .

Deshmane et al.<sup>17</sup> have examined this varying behavior in PP and PE-HD matrix by Izod impact strength measurements and have come to the conclusion that clay provides stronger interactions with PP, which results in increase or steadiness of the impact strength after clay incorporation, whereas because of the weaker PE-clay interaction, impact strength decreases notably in PE-HD matrix when clay is added. Deshmane et al. did not include any adhesion promoter in their studies, so relevance to its effects was not available.

### Morphology and nanoclay dispersion

The XRD measurements and the TEM analysis were carried out on all compounds containing clay in both matrices. Figure 9 illustrates the obtained interlayer spacing values at various clay concentrations and clay/adhesion promoter combinations in PP matrix. The interlayer spacing of pure Nanomer I.44P (MMT) is also included for reference. Figure 9 shows that the compounds containing Licomont have

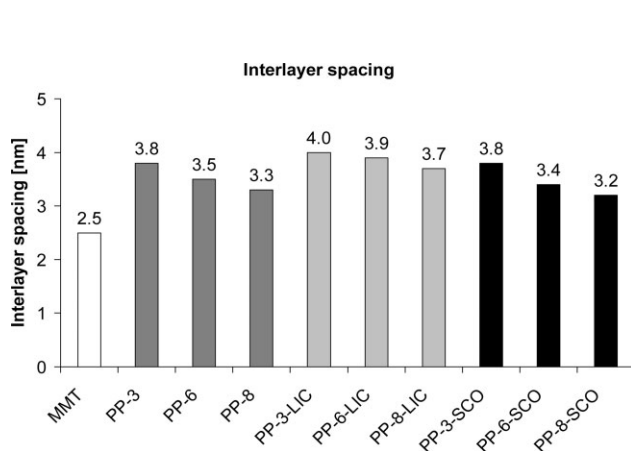


**Figure 9** Interlayer spacing values for the PP-based nanocomposites with pure MMT as a reference.

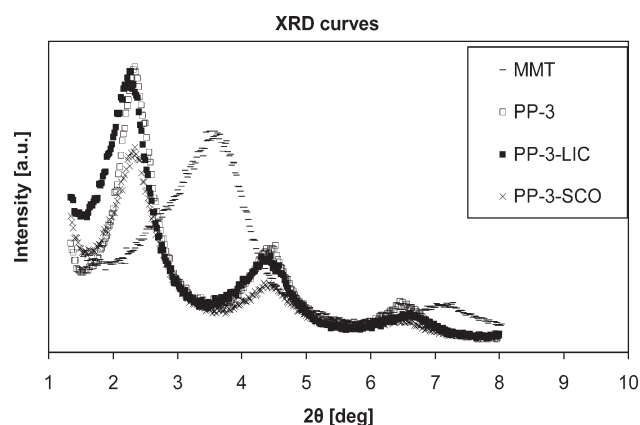


**Figure 10** XRD curves for the PP-based nanocomposites at a clay loading of 3 wt %. Pure MMT is included for reference.



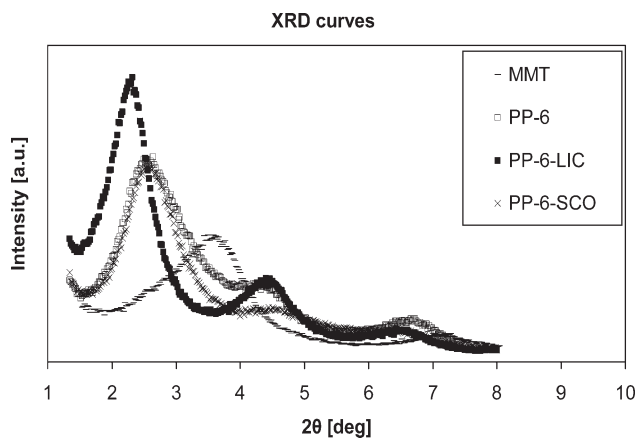


**Figure 11** XRD curves for the PP-based nanocomposites at a clay loading of 6 wt %. Pure MMT is included for reference.

higher interlayer spacing than compounds containing Scona. These findings support the results obtained in mechanical tests, i.e., a higher Young's

modulus achieved with Licomont use. It is obvious that a lower molecular weight adhesion promoter (Licomont) has easier access between the individual clay platelets than its higher molecular weight counterpart (Scona). This leads to more pronounced intercalation and most likely also to stronger adhesion between the nanoclay and the PP matrix because of the higher maleic anhydride content of Licomont. The interlayer spacing values of the compounds containing Licomont remain at a high level even when the filler content increases to 8 wt %. In turn, the interlayer spacing values for the Scona-containing compounds decrease more rapidly as a function of clay content, which is an indication of its poorer access between the silicate layers because of its higher molecular weight. Similar observations have been reported, for instance, by Svoboda et al.<sup>19</sup>

The XRD curves for compounds containing 3 wt % and 6 wt % of clay in PP matrix are illustrated in Figures 10 and 11, and the corresponding TEM images in Figures 12(a–d) and 13(a–c), respectively.

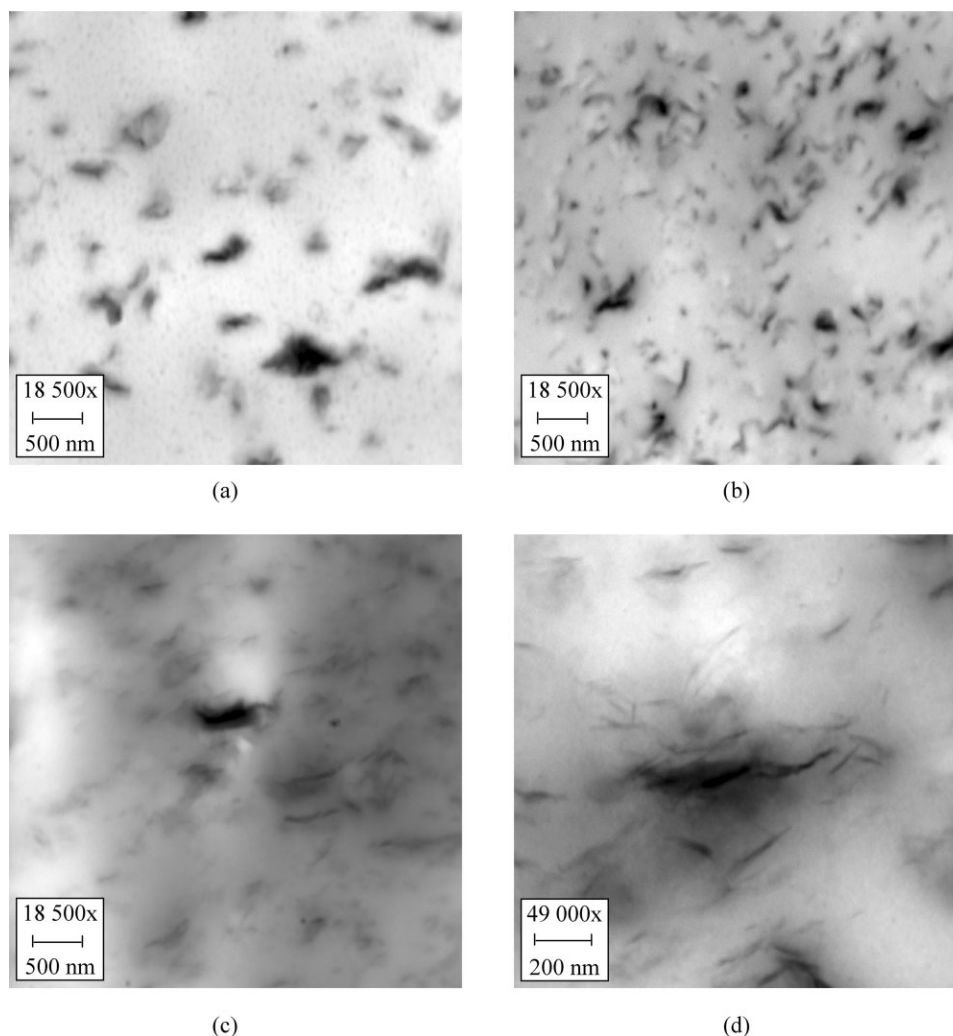


**Figure 12** TEM images of the PP-based nanocomposites at a clay loading of 3 wt %: a) PP-3 18,500 $\times$ , b) PP-3-LIC 18,500 $\times$ , c) PP-3-SCO 18,500 $\times$ , and d) PP-3-SCO 49,000 $\times$ .

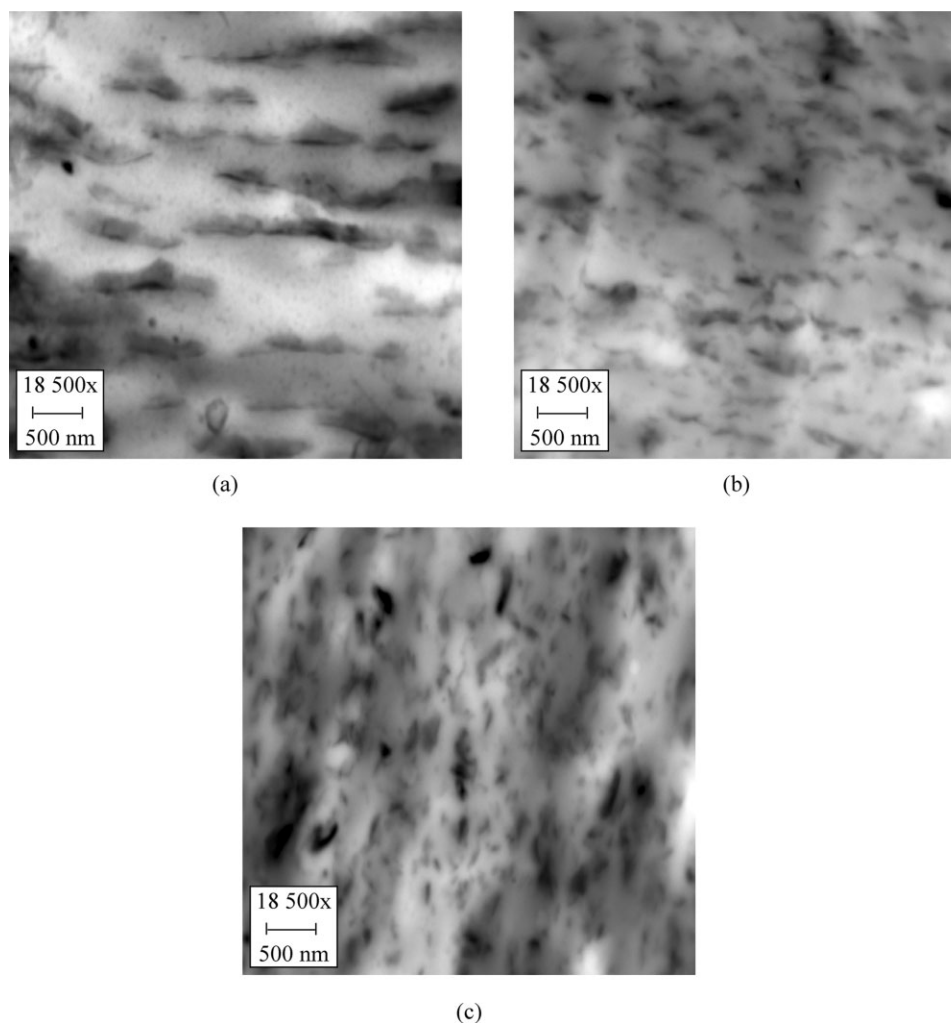


**Figure 13** TEM images of the PP-based nanocomposites at a clay loading of 6 wt %: a) PP-6 18,500 $\times$ , b) PP-6-LIC 18,500 $\times$ , and c) PP-6-SCO 18,500 $\times$ .

It can be seen from Figure 10 that the shape and size of the XRD curve is quite similar for compounds containing mere clay (PP-3) and clay with Licomont (PP-3-LIC). However, by comparing Figure 12(a,b), it is evident that dispersion and intercalation level are substantially better in case of PP-3-LIC than PP-3. On the other hand, the main peak for PP-3-SCO that appears at lower intensities and peaks at higher measuring angles are smaller compared with the others. The absence of peaks at high measuring angles is an indicator of a structure having few agglomerates. This is confirmed by Figure 12(c) in which only one larger agglomerate is visible accompanied by a great amount of highly dispersed and exfoliated clay particles. Higher variation in particle size is typical of high molecular weight adhesion promoters such as Scona, i.e., the nanocomposite structure includes finely dispersed clay particles together with larger clay stacks and agglomerates. The same type of morphology in the presence and absence of varying molecular weight adhesion pro-

motors in compounds containing 2 wt % of clay or 2 wt % of clay and 4 wt % of adhesion promoter is presented by Perrin-Sarazin et al.<sup>6</sup> Partial exfoliation from a larger clay particle can be seen in more detail in Figure 12(d).

At 6 wt % clay concentration, the peak for PP-6-LIC is still intense and narrow, and appears at lower angles than for the other two compounds (PP-6 and PP-6-SCO), as seen in Figure 11. This is an indication of strong and even intercalation as well as good dispersion, which are also confirmed by Figure 13(b). However, the sharp peak indicates only intercalation and probably not significant exfoliation in the composite: strong and even intercalation results after the successful penetration of the adhesion promoter between the silicate layers, but the polymer matrix has probably not accessed the clay galleries because there are no proper signs of exfoliation. For instance, results obtained by Perrin-Sarazin et al.<sup>6</sup> support this finding. In addition, there still appears a small peak around 4.5 $^{\circ}$ , which suggests presence of some

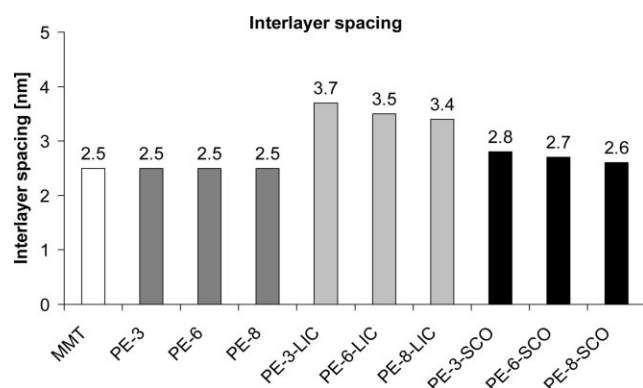


**Figure 14** Interlayer spacing values for the PE-HD-based nanocomposites with pure MMT as a reference.

agglomerates. For PP-6 and PP-6-SCO, the main peaks of the XRD curves are broader and shift to higher angles compared to PP-6-LIC. Wider particle size distribution leads to the broadening of the main peak, and shifting to higher angles reveals the weakening of intercalation. The lower intensity accompanied by the broadening of the peak can be a sign of partial exfoliation, which means that in addition to the adhesion promoter, the matrix polymer has also access between the silicate layers leading to partial exfoliation of clay. High molecular weight adhesion promoter has a more difficult access between the clay layers and poorer compatibility with the clay because of its lower maleic anhydride content, but on the other hand, it might have better compatibility with the matrix leading to higher exfoliation degree.<sup>6,15,20</sup> These observations show that PP-6 and PP-6-SCO have more irregular dispersion than PP-6-LIC; however, the peak at  $4.5^\circ$  vanishes in case of PP-6-SCO, which suggests that it does not include any major agglomerates in its structure. In fact, the major differences in dispersion level between PP-6 and PP-6-SCO can be easily detected from Figure 13(a,c). It is clear that the dispersion level of PP-6-SCO is more comparable to PP-6-LIC than to PP-6. The potential reasons for Licomont's better efficiency in mechanical property enhancement are then more pronounced adhesion because of its higher maleic anhydride content and more uniform dispersion, although the gained exfoliation level is lower than when Scona is used.

The interlayer spacing values reached in the PE-HD-based nanocomposites are presented in Figure 14. The values are notably lower than in the PP-based nanocomposites because of the strong hydrophobicity of polyethylene accompanied by high viscosity, i.e., low melt flow rate of the used PE-HD matrix. Satisfying intercalation degrees are only achieved with the use of Licomont; otherwise the interlayer spacing value stays near the level of pure MMT reference.

XRD curves for the PE-HD-based compounds containing 3 wt % of clay (Fig. 15) also reveal that intercalation degree is the highest when Licomont is used. The main peak of the curve (PE-3-LIC) has a long tail at small angles, which is referable to strong intercalation and also partial exfoliation. The exceptionally strong intercalation level can also be observed from the corresponding TEM image [Fig. 16 (b)]. Similar findings of partial exfoliation according to the shape of the XRD curve have been reported by Lee et al.<sup>11</sup> and Gopakumar et al.<sup>14</sup> The XRD curve of the compound containing mere clay (PE-3) follows the path of pure MMT reference. It also has a clear peak at higher measuring angles (around  $7^\circ$ ). Even though the interlayer spacing value obtained with compound PE-3-SCO is relatively near the value of PE-3 and MMT reference, the shape and size of the XRD curve is clearly different. One specific characteristic is the absence of peaks at high measuring angles for both PE-3-SCO and PE-3-LIC, which indicates that elimination of large agglomerates has been successful during the nanocomposite formation process. By comparing Figure 16(a,c), it is easily noticeable that intercalation level in the compound containing Scona is higher than that for the compound containing mere clay: when no adhesion promoter is used, clay particles have dispersed into smaller units, but intercalation is still poor.

Corresponding XRD curves at 8 wt % clay concentration are presented in Figure 17, and the relevant TEM images in Figure 18(a–c) at a magnification of 20,000 and in Figure 19(a–c) at a magnification of 80,000. The shape of the XRD curves for compounds that contain adhesion promoters change notably compared with the curves at 3 wt % clay concentration, whereas the curve for PE-8 is somewhat similar to that for PE-3 in Figure 15. The tail at low measuring angles disappears for PE-8-LIC and also a flat

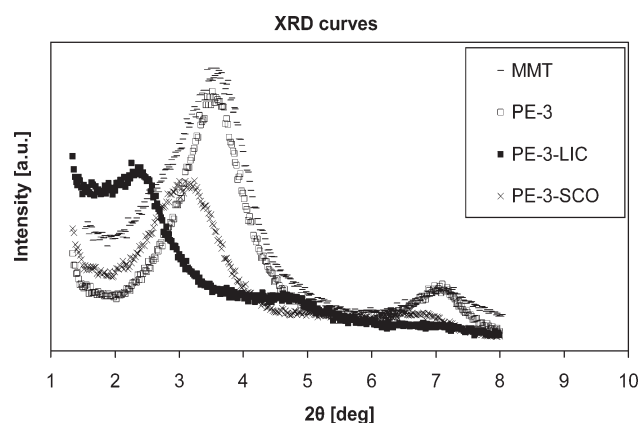


**Figure 15** XRD curves for the PE-HD-based nanocomposites at a clay loading of 3 wt %. Pure MMT is included for reference.

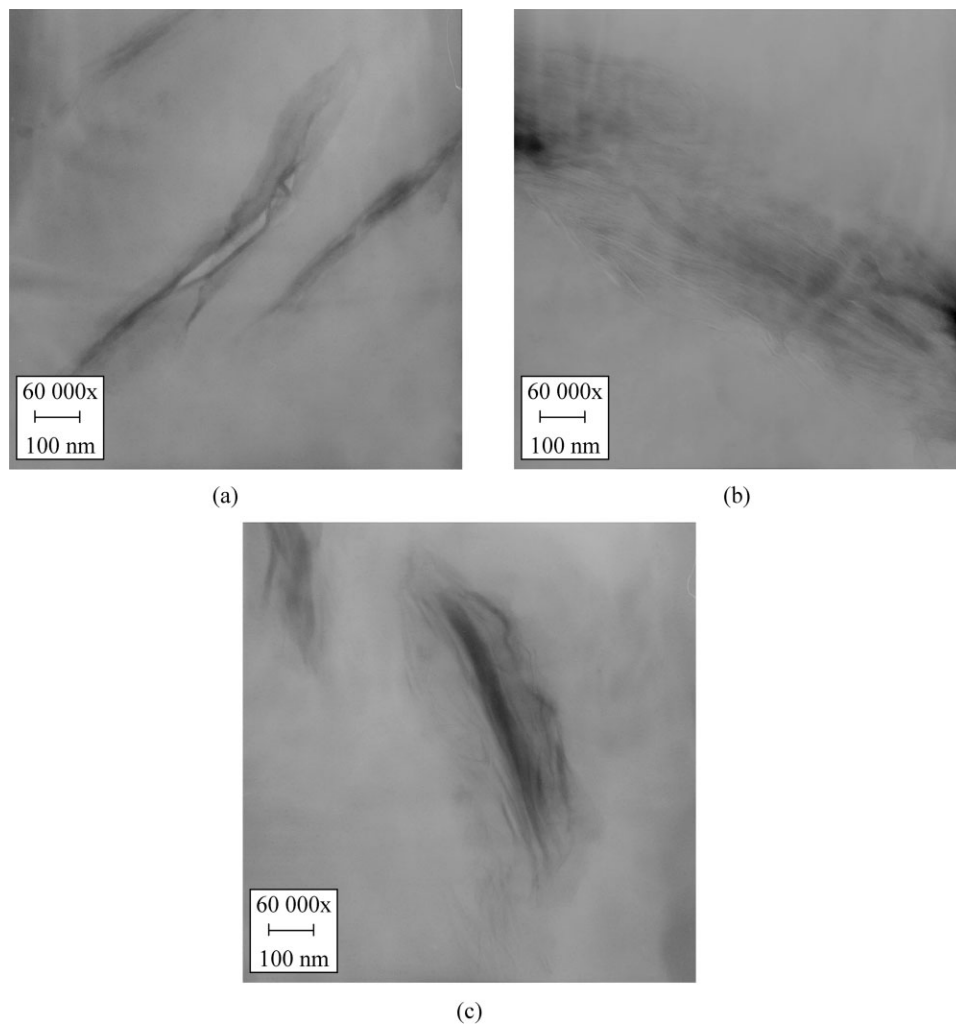


**Figure 16** TEM images of the PE-HD-based nanocomposites at a clay loading of 3 wt %: a) PE-3 60,000 $\times$ , b) PE-3-LIC 60,000 $\times$ , and c) PE-3-SCO 60,000 $\times$ .

broad peak strengthens around 5 $^{\circ}$ , which suggest a weakening intercalation and an increasing formation of agglomerates. The more compact stacking of sili-

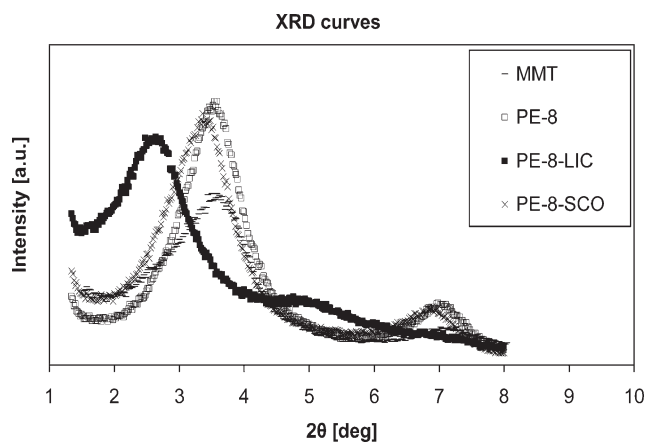


**Figure 17** XRD curves for the PE-HD-based nanocomposites at a clay loading of 8 wt %. Pure MMT is included for reference.

cate layers at higher clay loading is clearly detectable by comparing Figures 16(b) and 19(b). The same type of behavior was also noticed by Lee et al.<sup>11</sup> at a higher clay concentration. In turn, the XRD curve for PE-8-SCO approaches the path of PE-8, including also a peak at 7 $^{\circ}$  revealing the formation of agglomerates, whereas the behavior for the corresponding compounds at 3 wt % clay concentration was quite different. However, differences in morphology are still evident when comparing Figures 18(a,c) and 19(a,c). Mere clay addition results in poorly intercalated clay stacks, whereas the implementation of Scona leads to distinct intercalation and also partial exfoliation. According to TEM images [Figs. 18(a-c), 19(a-c)], the intercalation and dispersion of PE-8-SCO seems to be closer to that of PE-8-LIC than PE-8. For instance, Osman et al.<sup>21</sup> have reported that stiffness, i.e., Young's modulus is more pronounced in PE-HD matrix when strong intercalation and partial exfoliation occurs, which is in good accordance with our results: the increase of Young's modulus

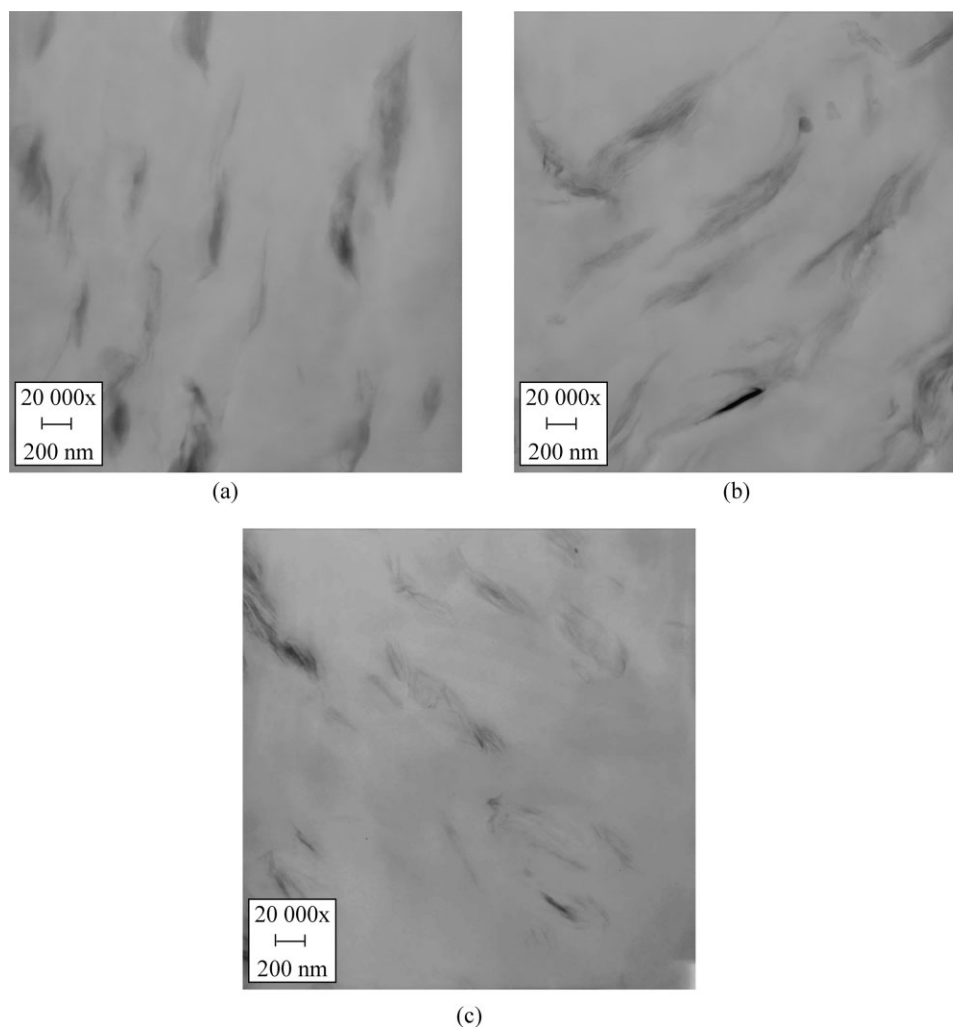


**Figure 18** TEM images of the PE-HD-based nanocomposites at a clay loading of 8 wt %: a) PE-8 20,000 $\times$ , b) PE-8-LIC 20,000 $\times$ , and c) PE-8-SCO 20,000 $\times$ .

was more evident when Licomont or Scona was used compared with mere clay addition, which also resulted in more poorly intercalated and exfoliated composites proven by the TEM images.

### CONCLUSIONS

The performance of PP-g-MA-based adhesion promoters is strongly related to their functionality, i.e., maleic anhydride content, which relates to their adhesion capability with the clay filler and the compatibility with the used polyolefin matrix. In this study, the low molecular weight adhesion promoter (Licomont) yielded more pronounced enhancements in intercalation degree in both PP and PE-HD matrix because of its easier access between the silicate layers. On the other hand, the use of higher molecular weight adhesion promoter (Scona) led to a more uneven dispersion but also established strongly exfoliated particles. More pronounced property enhancements were achieved with the use of Licomont, for

its higher maleic anhydride content enabled intense adhesion with clay. This strong adhesion accompanied by the obtained high intercalation level and even dispersion assured a distinct effect on mechanical properties in both matrices.

In PP matrix, the enhancements in Young's modulus were modest when the high molecular weight adhesion promoter (Scona) was used. On the other hand, the effect on impact strength was of the same magnitude as with the use of Licomont. The weaker efficiency of Scona in PP matrix was probably because of its lower maleic anhydride content, impairing possibilities of strong adhesion to the filler and higher molecular weight hindering proper penetration of polymer chains into the clay galleries. Even though exfoliation is on a higher level when Scona is used, its low maleic anhydride content does not enable similar adhesion as with the use of Licomont, resulting in a lower impact on modulus. In PE-HD matrix, the efficiency of both adhesion promoters was similar indicating that in case of the

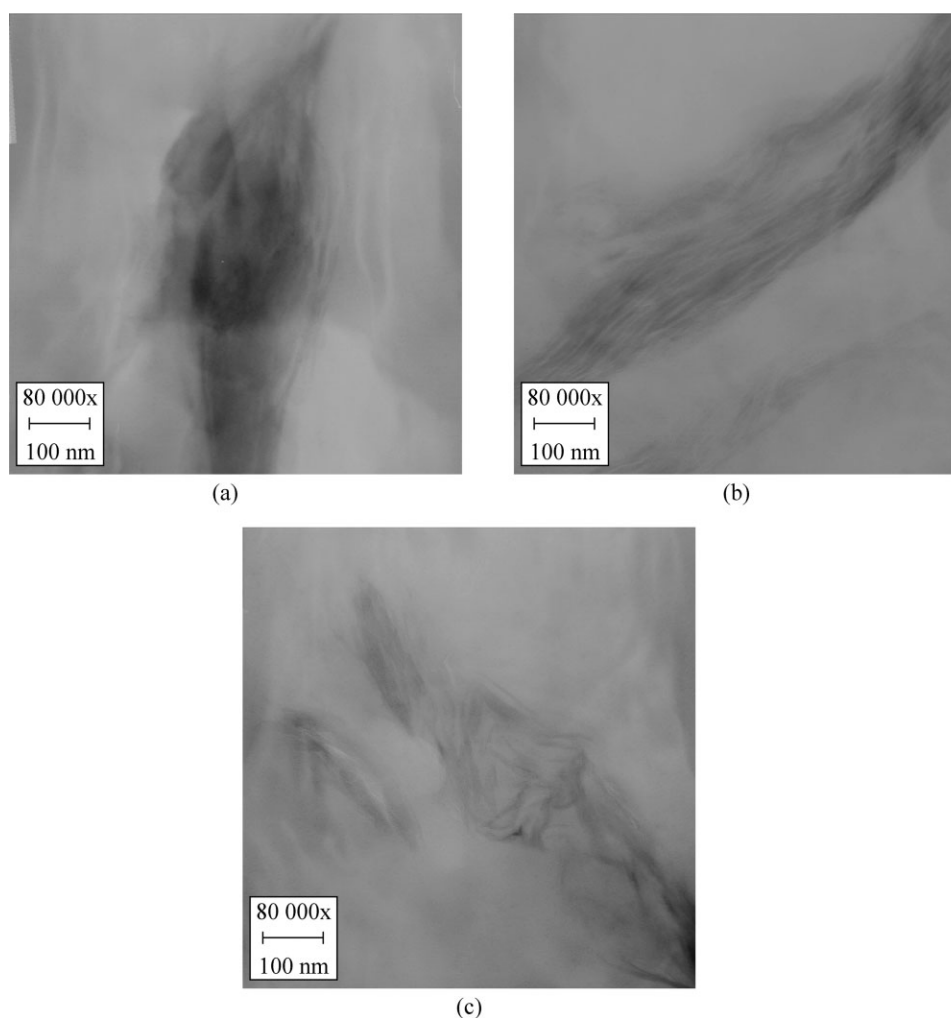


**Figure 19** TEM images of the PE-HD-based nanocomposites at a clay loading of 8 wt %: a) PE-8 80,000 $\times$ , b) PE-8-LIC 80,000 $\times$ , and c) PE-8-SCO 80,000 $\times$ .

chosen PE-HD matrix, neither the maleic anhydride content nor the molecular weight of the adhesion promoter played a crucial role in relation to the gained enhancements in mechanical properties.

In general, the effect of higher maleic anhydride content of the adhesion promoter was more intense in relation to gained property enhancements than the effect of its molecular weight. Molecular weight seemed to influence highly on the level of clay intercalation and exfoliation, but the efficiency of adhesion was clearly comparable to the content of maleic anhydride, which in turn seemed to determine the level of mechanical property enhancements. The lower molecular weight of Licomont resulted in a high intercalation level and even dispersion in both matrices, and also led to more pronounced property enhancements because of its high adhesion capability. Clay was more intensely exfoliated with the use of the high molecular weight adhesion promoter (Scona) but still, the gained property enhancements were not necessarily on the same level because of

the lack of adhesion induced by its lower maleic anhydride content.

The authors would like to thank Janne Sundelin (Institute of Materials Science, Tampere University of Technology) for his efforts with the TEM analysis and the XRD measurements, as well as Mervi Lindman and Arja Strandell (Institute of Biomaterials Science, University of Helsinki) for the preparation of the TEM samples.

## References

1. Kawasumi, M.; Hasegawa, N.; Kato, M.; Usuki, A.; Okada, A. *Macromolecules* 1997, 30, 6333.
2. Kato, M.; Usuki, A.; Okada, A. *J Appl Polym Sci* 1997, 66, 1781.
3. Hasegawa, N.; Kawasumi, M.; Kato, M.; Usuki, A.; Okada, A. *J Appl Polym Sci* 1998, 67, 87.
4. Ton-That, M.-T.; Perrin-Sarazin, F.; Cole, K. C.; Bureau, M. N.; Denault, J. *Polym Eng Sci* 2004, 44, 1212.
5. Wang, Y.; Chen, F.-B.; Li, Y.-C.; Wu, K.-C. *Comp Part B Eng* 2004, 35, 111.
6. Perrin-Sarazin, F.; Ton-That, M.-T.; Bureau, M. N.; Denault, J. *Polymer* 2005, 46, 11624.

7. Reichert, P.; Nitz, H.; Klinke, S.; Brandsch, R.; Thomann, R.; Mülhaupt, R. *Macrom Mater Eng* 2000, 275, 8.
8. Jordan, J.; Jacob, K. I.; Tannenbaum, R.; Sharaf, M. A.; Jasiuk, I. *Mater Sci Eng A* 2005, 393, 1.
9. Lomakin, S. M.; Dubnikova, I. L.; Berezina, S. M.; Zaikov, G. E. *Polym Int* 2005, 54, 999.
10. Gorrasi, G.; Tammara, L.; Tortora, M.; Vittoria, V.; Kaempfer, D.; Reichert, P.; Mülhaupt, R. *J Pol Sci Part B Pol Phys* 2003, 41, 1798.
11. Lee, J.-H.; Jung, D.; Hong, C.-E.; Rhee, K. Y.; Advani, S. G. *Comp Sci Tech* 2005, 65, 1996.
12. Wunderlich, B. *Thermal analysis*, Academic Press: New York, 1990.
13. Wunderlich, B. *Macromolecular Physics*, Vol. 3, Crystal Melting, Academic Press: New York, 1980.
14. Gopakumar, T. G.; Lee, J. A.; Kontopoulou, M.; Parent, J. S. *Polymer* 2002, 43, 5483.
15. Modesti, M.; Lorenzetti, A.; Bon, D.; Besco, S. *Polymer* 2005, 46, 10237.
16. Ding, C.; Jia, D.; He, H.; Guo, B.; Hong, H. *Polymer Test* 2005, 24, 94.
17. Deshmane, C.; Yuan, Q.; Perkins, R. S.; Misra, R. D. K. *Mat Sci Eng A* 2007, 458, 150.
18. Li, P.; Song, G.; Yin, L.; Wang, L.; Ma, G. *J Appl Polym Sci* 2008, 108, 2116.
19. Svoboda, P.; Zeng, C.; Wang, H.; Lee, L. J.; Tomasko, D. L. *J Appl Polym Sci* 2002, 85, 1562.
20. Lertwimolnun, W.; Vergnes, B. *Polymer* 2005, 46, 3462.
21. Osman, M. A.; Rupp, J. E. P.; Suter, U. W. *Polymer* 2005, 46, 8202.